Optimization of Jet Mixer Geometry and Mixing Studies

A. Egedy[1*], B. Molnar[1], T. Varga[1], T. Chován[1]
[1]University of Pannonia Department of Process Engineering,
*10th Egyetem Str. Veszprém, Hungary, H-8200, egedya@fmt.uni-pannon.hu

Abstract: Mixing is one of the most crucial operation in process industry. Jet mixing has become an alternative to mechanical mixing for various applications. q, like in case of other mixing devices, is to increase the heat and mass transfer between the phases. Beside the injection position the geometry of the jet mixer and the injection nozzle has a major effect on the injection. In our study COMSOL Multiphysics software was used to carry out the experimental and simulation of the different jet geometries. The jet mixer was placed in a tube which was used to homogenize the chemical components in a very short reaction zone. The mixing must be completed by the end of the reaction zone because incomplete mixing will lead to side reactions in the investigated case study.

Keywords: jet mixing, COMSOL MATLAB Livelink, residence time, particle tracing

1. Introduction

Mixing is one of the widely used and studied operations. However, there is still a lot of uncovered parts in this field. Research projects are going on to understand, and describe the inner flow field of the industrial devices, and to support the flow field based design and operation.

CFD simulators can be used for the modeling the inner flow field in chemical reactors. With the help of CFD simulators engineers can achieve better understanding on the operation of chemical reactors, e.g. the well mixed zones and dead zones can be found. CFD simulators can be useful in new technology design. Inlet positions, rotational speeds and other design and operation parameters can be optimized, without creating any physical device.

In this study dispersers are examined based on different point of view. The dispersers are mixers, where the injected gas or liquid stream mixed the fluid. Dispersers are widely used, mostly in cases where highly exothermic reactions take place. The partial injection of the dangerous reagent can be an excellent way to control the reaction, which will lead to the proper product and safe operation.

Dispersers are used to:

- prevent thermal runaway in stirred reactors with inhibition techniques [1],
- in engines, for fuel injection,
- mixing crude oil in storage tanks [2],
- precipitation of nanoparticles [3],
- waste management [4].

These technologies can be difficult to study in conventional methods, due to the lack of experimental results. With using a CFD simulator, the model of the physical system can be implemented, and the mixing efficiency of dispersers can be calculated. Structural and operating parameters can be examined, e.g. nozzle design, and injection position, or flow rates. [5].

The validation of the implemented CFD model can be as challenging as the model building. There are multiple methods to validate the CFD model, mostly using some tracing material injected to the system. Based on the detection the measurement can be:

- Residence time measurement [6] can be used in continuous devices. It mostly uses conductometry and photometrical methods for concentration measurements.
- Mixing time measurements [7] are mostly used in batch reactors, using dye injections or acid-base reaction. Mixing time is by the definition the time needed for a system to achieve a predefined level of homogeneity.
- Chemical reaction [4] with injection.

The homogeneity of the system can be measured with opalescence measurement device [8]. Video processing based validation can be applied if the device is transparent. The greatest advantage of video processing methods is the excellent reproducibility, and it can be a great visualization tool too (e.g. with dye homogenization). The most interesting step in these techniques is the image processing step, where the homogeneity changes can be followed within the reactor. There are several studies in the field of video processing based model validation using mixing time measurements [9-

11]. Injection and homogenization can be followed with using dye injection techniques [4, 5, 6].

In this study different disperser nozzles were compared based on mixing effectiveness. Apart from the simulation studies a measurement system was designed and built, which can be used for model validation using different experiments. The model validation was completed with homogeneity measurements using dye injection. Based on the results an optimal nozzle configuration was proposed.

2. Experimental methods

A measurement system was built to validate the CFD model. The experimental device contains the disperser with two inlets, and the nozzles created with a fast prototype producing device (Mendelmax 2.0), based on CAD drawings. The experimental apparatus contains two concentric pipes, an injection nozzle, two inlets and one outlet.

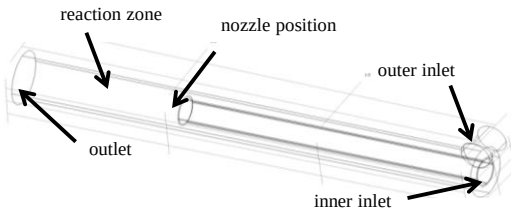

Figure 1. The used experimental disperser device

Eight different nozzles were applied, with number of holes from four up to ten, and straight and swirled holes too. Figure 1 shows the experimental device, and Figure 2 shows the investigated nozzles.

Dye injection experiments were performed with three inlet flow rates, using neutral red indicator. The change in homogeneity of the system was detected and recorded using a HD camera (Sony CX115E). Three different experiments were completed for each disperser nozzle all with 90 l/h inner flow rate and 210, 135 and 0 l/h outer flow rate. Altogether 24 different measurements were performed. Water was applied for material, because in case of dye injections only a diluted solution of the dye was presented in the system. Then the results were evaluated, and the experimental results were compared to each other, and to the simulation results.

Figure 2. The applied nozzles first row - straight design, second row - swirled design

A simple algorithm was used for evaluate the experimental results. The three color (R,G,B) videos were averaged frame by frame. A background was created based on the frames not containing dye (in the first 25 frames). Then every frame was compared to this background, and a summarized difference value was calculated. The data was normalized based on the maximum value of the difference. Then we found the first value when the difference is below 0.05 (t_{95} 95% homogeneity). The difference based residence time was defined as the difference between the maximum value, and t_{95} [9].

3. The developed CFD model

The full 3D model of the disperser was implemented in COMSOL Multiphysics.

There are several processes have to be modeled: a turbulent k-ε model for momentum balance and component mass balances. Eq 1 is the continuity equation, and Eq 2 is the Navier Stokes equation. Eq 3 and Eq 4 describe the turbulent kinetic energy and the turbulent dissipation rate, while Eq 5 and Eq 6 calculate the turbulent viscosity, and the stress tensor.

$$\rho(u \cdot \nabla)u = \nabla \cdot \left[\rho l + (\mu + \mu_T)(\nabla u + (\nabla u)^T) - \frac{2}{3}(\mu + \mu_T)l - \frac{2}{3}\rho k l\right] + F \quad (1)$$

$$\nabla \cdot (\rho u) = 0 \quad (2)$$

$$\rho(u \cdot \nabla)k = \nabla \cdot \left[\left(\mu + \frac{\mu_T}{\sigma_k}\right)\nabla k\right] + P_k - \rho\varepsilon \quad (3)$$

$$\rho(u \cdot \nabla)\varepsilon = \nabla \cdot \left[\left(\mu + \frac{\mu_T}{\sigma_e}\right)\nabla \varepsilon\right] + c_{e1}\frac{\varepsilon}{k}P_k - c_{e2}\rho\frac{\varepsilon^2}{k} \quad (4)$$

$$\mu_T = \rho c_\mu \frac{k^2}{\varepsilon} \quad (5)$$

$$P_k = \mu_T\left[\nabla u: (\nabla u + (\nabla u)^T - \frac{2}{3}(\nabla \cdot u)^2\right] - \frac{2}{3}\rho k \nabla \cdot u \quad (6)$$

The following boundary conditions were applied in the solution of the momentum balance:

- Velocity inlet in the inner and outer inlet boundaries,
- a pressure no viscous stress boundary for the outlet boundary,
- wall boundary condition with no slip for all of the other boundaries.

The momentum balance was calculated in a stationary study because only a short time needed to a stationary momentum balance after changes in operation parameters. A component balance (Eq 7) was built in, for calculating the residence time inside the reactor containing the convective, conductive, and the source terms. In case of residence time distribution simulation the source term was neglected.

$$\nabla \cdot (-D_i \nabla c_i) + u \cdot \nabla c_i = R_i \quad (7)$$

The following boundary conditions were applied in the solution of the component balance:

- Concentration inflow in the inner inlet boundary,
- outflow boundary in the outlet,
- insulation boundary condition with no slip for all of the other boundaries.

The dye injection was described using a rectangle function centered at 2 s in a time dependent study. The concentration changes were detected in time, and a surface integral was calculated at the outlet boundary.

Beside the component balance calculation a particle tracing study were also performed. Flow field based particle tracing was used and approximately 900 particles were injected to the disperser to both inlets in a time dependent study in a mesh based release. The movement of a particle (Eq 8) can be calculated by computing drag (Eq. 9-10) and gravity (Eq. 11) forces. The different parameters and nozzle configurations were evaluated with Poincare plots displayed at the outlet boundary. The particles from different inlets were displayed with different color, and the mixing efficiency was evaluated based on these Poincare plots, displaying the mixing between particles from different inlets.

$$\frac{d(m_p v)}{dt} = F_t \quad (8)$$

$$F = \frac{1}{\tau_p} m_p (u - v) \quad (9)$$

$$\tau_p = \frac{\rho_p d_p^2}{18\mu} \quad (10)$$

$$F = m_p g \frac{\rho_p - \rho}{\rho_p} \quad (11)$$

A mesh independence study was also performed for the system. Four different types of mesh were applied (coarser, coarse, normal, finer) and the meshes were evaluated based on computation time, and balance error. Figure 3 shows the results of the mesh independence study.

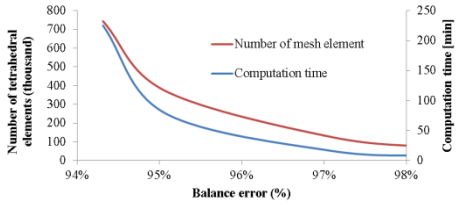

Figure 3. The results of the mesh independence study

As Figure 3 shows the higher the number of the mesh elements, the higher the computation time. Besides higher mesh number means lower balance goodness, so the coarse mesh category was chosen for the calculation of the model. Figure 4 shows an example of the implemented mesh, in case of the straight four-hole nozzle at the neighborhood of the nozzle.

MATLAB Livelink was used for the coupled momentum-component balances calculation using cycles, and the values of integrated concentrations are computed in a time dependent study. There are 20 different nozzle constructions from 1°to 20° in the simulation studies. The particle tracing simulations were conducted in individual simulations.

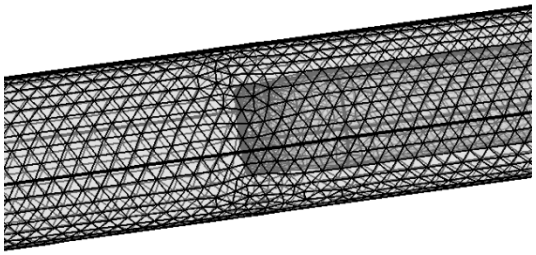

Figure 4. An example for the applied mesh in case of four-hole nozzle

An Intel Xeon W3530 computer was used for the residence time simulation studies resulting approximately 25 minutes calculation time. An Intel Xeon E5620 computer was used for the particle tracing simulation studies resulting approximately 10 minutes calculation time in case of momentum balance and 10 minutes s calculation time in case of particle tracing simulations.

3. Results

Stationary momentum balance was calculated as the first step in both simulation studies. Figure 5a shows the developed velocity field inside the reactor, and Figure 5b is the streamline plot based on the results. The red streamlines has a starting boundary of the inner inlet, the black ones start from the outer inlet.

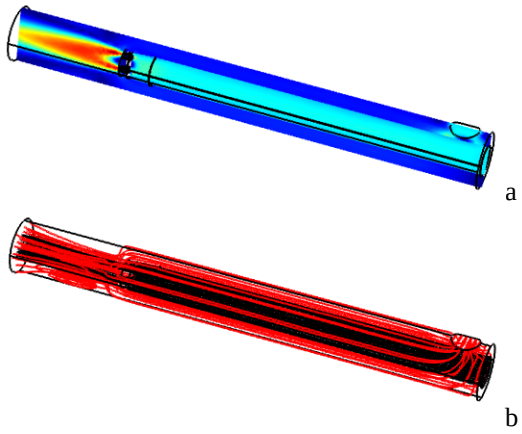

Figure 5. a The velocity field inside the disperser [m/s] (rainbow color bar), b streamlines inside the reactor red- inner inlet started streamlines, black – outer inlet started streamlines (4 hole nozzle).

Identical inlet velocities were applied for both inlets. As Figure 5a shows there is a maximum velocity near the nozzle outlets, and the average velocity is higher in the inner tube, than the outer.

The first set of the simulation experiments was the residence time analysis in time dependent studies. A fixed amount of dye was injected to the inner inlet using a rectangle function (2 s).

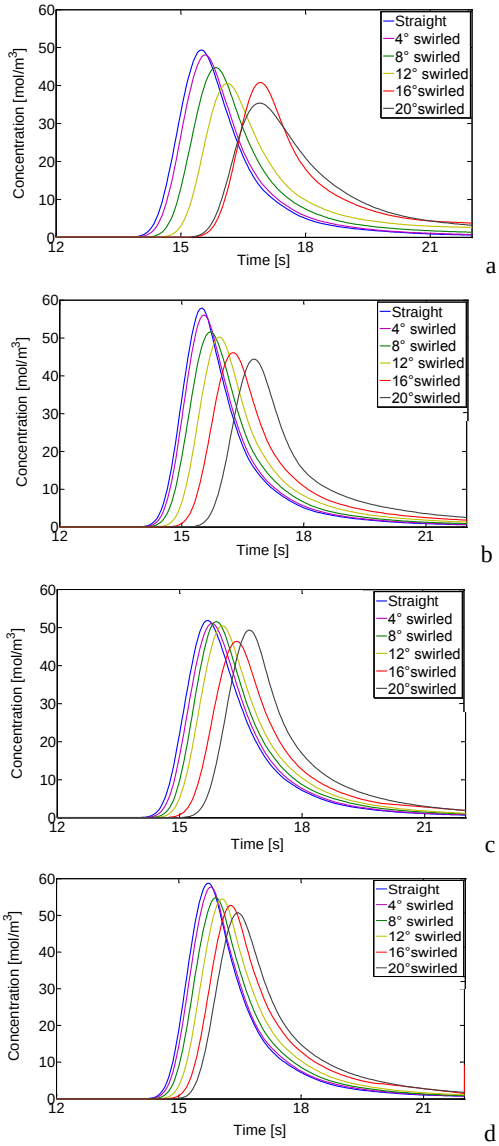

Figure 6. The results of the residence time simulation – integrated concentrations on the outlet boundary a four-hole nozzle, b six-hole nozzle, c eight-hole nozzle, d ten-hole nozzle

All four nozzle numbers were examined, and simulation studies were performed with different

angle of holes. Figure 6 shows the results curves with the different cases from 4-10 holes (Figure 6 a-d).

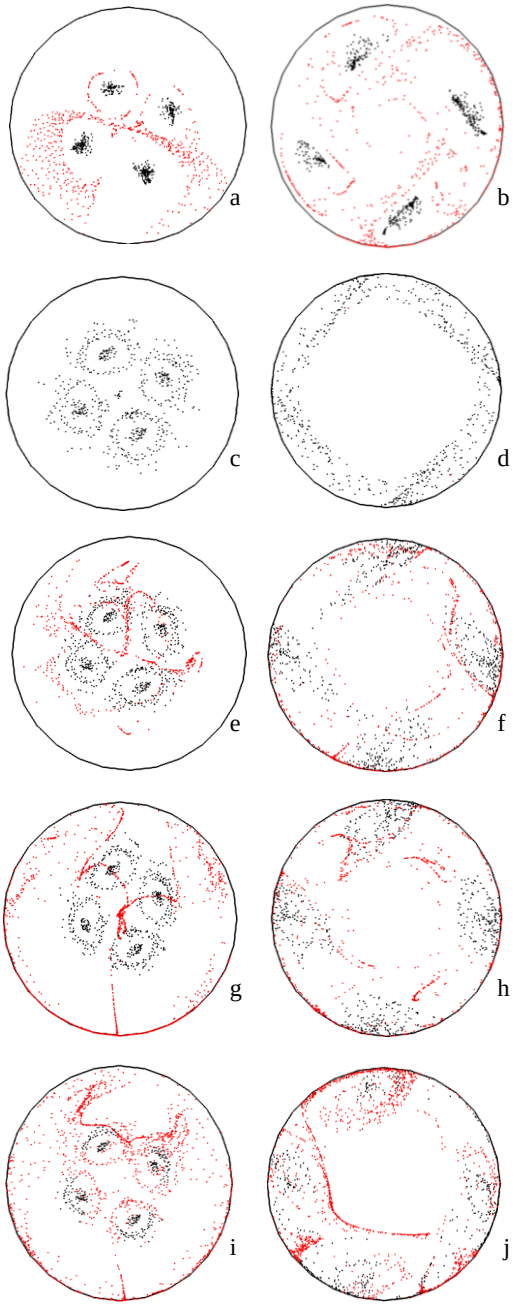

Figure 7. Poincare plots of the particle tracing simulations (different flow rates with four-hole construction)

The residence time is higher with increasing degree of swirl. The interval between the most swirled and the straight case become lower with increasing number of holes.

The next simulation study was particle tracing. Different flow rates were applied in the first study. Figure 7 shows the results with four-hole disperser. The black points shows the particles originated from the inner inlet, and the red points shows the particles originated from the outer inlet. The pictures on the left (a, c, e, g, i) shows the straight and the pictures on the right (b, d, f, h, j) shows the swirled hole cases.

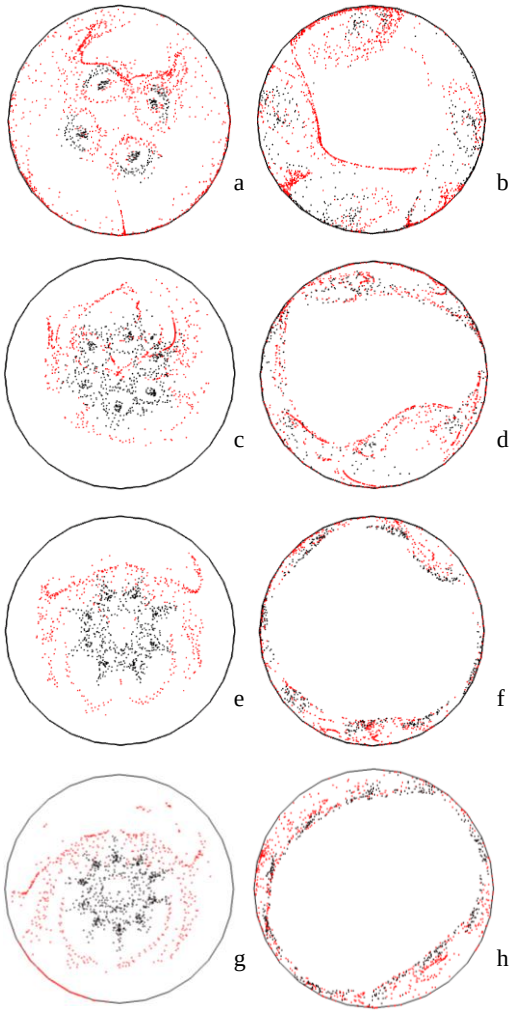

Figure 8. Poincare plots of the particle tracing simulations (different constructions with constant flow rate 180 l/h equal)

In cases of a and b the full flow rate is 44 l/h and the two inlets has equal flow rate. In case of c and d the fluid flows only through the inner

inlet with 90 l/h. In e and f the full flow rate is 180 l/h and the two inlets has equal flow rate. In cases g and h the inner flow rate is 90 l/h and the outer flow rate is 135 l/h. In cases i and j the inner flow rate is 90 l/h and the outer flow rate is 210 l/h. As the Figure 7 shows the higher the flow rate the better the mixing efficiency, and the swirled cases make the vessel more mixed. Figure 8 shows the results with different number of holes (a,b-4-hole, c,d-6 hole, e,f-8 hole, g,h-10 hole).

The higher number of holes leads to better mixing efficiency, and these experiments also show the positive effect of the swirled construction. However, in the swirled cases the well mixed areas are only concentrated near the walls.

Figure 9 shows the comparison of the experimental and simulation based residence times.

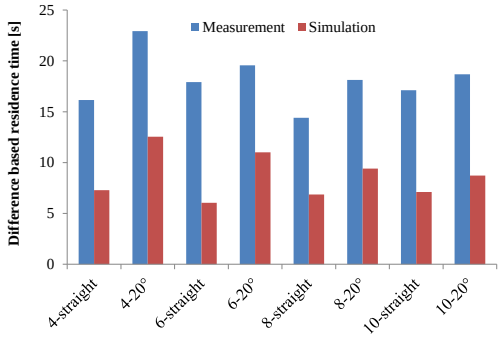

Figure 9. Model validation with the comparison of experimental and simulation results

There are qualitative similarities between the measurement and the simulation results. The tendencies are the same; however the numerical values are quite different. The next step of our research will be the identification of better model parameters which will lead to a model, which describes the physical system more adequately.

4. Conclusions

A detailed CFD model of a disperser was created. The model contains multiple equations describing the (momentum and component mass balances). Different simulation studies were performed including residence time distribution and particle tracing studies. The disperser configurations were evaluated based on the results and the swirled configurations were found better.

An experimental device was proposed and built, and the developed CFD model was validated based on residence time measurements. A good qualitative agreement was found between the experimental and simulation results.

In the future we are planning to find better model parameters for quantitative model validation.

5. Notation

Symbol	Description	Unit
p	Pressure	Pa
ρ	Density	kg/m^3
u	Velocity vector	m/s
μ	Dynamic viscosity	Pas
μ_t	Turbulent viscosity	Pas
k	Turbulent kinetic energy	m^2/s^3
ε	Turbulent energy dissipation	m^2/s^2
C_ε	Constant	1.3
$C_{\varepsilon 1}$	Constant	1.44
$C_{\varepsilon 2}$	Constant	1.92
C_μ	Constant	0.09
σ_k, σ_ε	Constant	1
t	Time	s
F	Force vector	N
P_k	Stress tensor	
c_i	Concentration	mol/m^3
D_i	Diffusion constant	m^2/s
τ_p	Slip stress	
m_p	Particle mass	kg
F_t	Force affect the particle	N
ρ_p	Particle density	kg/m^3
d_p	Particle diameter	m

6. References

1. Dakshinamoorthy, D., Khopkar, A.R., Louvar, J.F., Ranade, V.V, CFD simulation of shortstopping runaway reactions in vessels agitated with impellers and jets, *Journal of Loss Prevention in the Process Industries*, **19**, 570-581 (2006)

2. Rahimi, M., Parvareh, A., CFD study of mixing by coupled jet-impeller mixer sin a large crude oil storage tank, *Computers and Chemical Engineering*, **31**, 737-744 (2007)
3. Gavi, E., Marchisio D.L., Barresi, A.A., CFD modelling and scale-up of Confined Impinging Jet Reactors, *Chemical Engineering Science*, **62**, 2228-2241 (2007)
4. Parvareh, A., Rahimi, M., Yarmohammadi, M., Alsairafi, A.A., Experimental and CFD study on the effect of jet position on reactant disperion performance, International *Communications in Heat and Mass Trasfer*, **36**, 1096-1102 (2009)
5. Torré, J-P., Fletcher D.F., Lasuye, T., Xuereb, C., An experimental and CFD study of liquid jet injection into a partially baffled mixing vessel: A contribution to process safety by improving the quenching of runaway reactions, *Chemical Engineering Science*, **63**, 924-942 (2008)
6. Furman, L., Stegowski, Z., CFD models of jet mixing and their validation by tracer experiments, *Chemical Engineering and Processing: Process Intensification*, **50**, 300-304 (2011)
7. Patwardhan, A.W., CFD modeling of jet mixed tanks, *Chemical Engineering Science*, **57**, 1307-1318 (2002)
8. Rahimi, M., Parvareh, A., Experimental and CFD investigation on mixing by a jet in a semi-industrial stirred tank. *Chemical Engineering Journal*, **115**, 85-92, 2005
9. Egedy, A., Varga, T., Chován, T., CFD modelling and video based model validation for a stirred reactor, *Computer Aided Chemical Engineering*, 1123-1127 (2012)
10. Cabaret, F., Bonnot, S., Fradette, L., Tanguy, P.A., Mixing time analysis Using colorimetric methods and image processing, *Industrial Engineering Chemistry and Research*, **46**, 5032-5042 (2007)
11. Visuri, O., Laakkonen, M., Aittamaa, J., A digital imaging technique for the analysis of local inhomogenities from agitated vessels, *Chemical Engineering Technology*, **30**, 1692-1699 (2007)

7. Acknowledgements

This work was supported in the frame of the TÉT_12_RO-1-2013-0017 and TAMOP-4.2.2/A-11/1/KONV-2012-0071 projects. Tamás Varga's research activity in this work was supported by the European Union and the State of Hungary, co-financed by the European Social Fund in the framework of TÁMOP-4.2.4.A/ 2-11/1-2012-0001 'National Excellence Program'.